RESEARCH ARTICLE

# The Spirit Rover's Athena Science Investigation at Gusev Crater, Mars

S. W. Squyres,[1]* R. E. Arvidson,[2] J. F. Bell III,[1] J. Brückner,[3] N. A. Cabrol,[4] W. Calvin,[5] M. H. Carr,[6] P. R. Christensen,[7] B. C. Clark,[8] L. Crumpler,[9] D. J. Des Marais,[10] C. d'Uston,[11] T. Economou,[12] J. Farmer,[7] W. Farrand,[13] W. Folkner,[14] M. Golombek,[14] S. Gorevan,[15] J. A. Grant,[16] R. Greeley,[7] J. Grotzinger,[17] L. Haskin,[2] K. E. Herkenhoff,[18] S. Hviid,[19] J. Johnson,[18] G. Klingelhöfer,[20] A. Knoll,[21] G. Landis,[22] M. Lemmon,[23] R. Li,[24] M. B. Madsen,[25] M. C. Malin,[26] S. M. McLennan,[27] H. Y. McSween,[28] D. W. Ming,[29] J. Moersch,[28] R. V. Morris,[29] T. Parker,[14] J. W. Rice Jr.,[7] L. Richter,[30] R. Rieder,[3] M. Sims,[10] M. Smith,[31] P. Smith,[32] L. A. Soderblom,[18] R. Sullivan,[1] H. Wänke,[3] T. Wdowiak,[33] M. Wolff,[34] A. Yen[14]

The Mars Exploration Rover Spirit and its Athena science payload have been used to investigate a landing site in Gusev crater. Gusev is hypothesized to be the site of a former lake, but no clear evidence for lacustrine sedimentation has been found to date. Instead, the dominant lithology is basalt, and the dominant geologic processes are impact events and eolian transport. Many rocks exhibit coatings and other characteristics that may be evidence for minor aqueous alteration. Any lacustrine sediments that may exist at this location within Gusev apparently have been buried by lavas that have undergone subsequent impact disruption.

Spirit landed in Gusev crater on 4 January 2004 UTC. It was followed 21 days later by Opportunity, which landed on Meridiani Planum. Both vehicles landed using a variant of the airbag landing system that was developed for the Mars Pathfinder mission, deploying the rovers after the landers had come to rest on the surface (*1*). The primary scientific objective of their mission is to explore two sites on the martian surface where water may once have been present, and to assess past environmental conditions at those sites and their suitability for life. Here we provide an overview of the results from the 90-sol (*2*) nominal mission of Spirit.

Like Opportunity, Spirit carries a copy of the Athena science payload (*3*) (Fig. 1). The topography, morphology, and mineralogy of the scene around the rover have been revealed by two remote sensing instruments: a panoramic camera (Pancam) and a miniature thermal emission spectrometer (Mini-TES). Pancam (*4*) is a stereo camera whose filters provide 11 unique color spectral bandpasses over the spectral region from 0.4 to 1.1 mm, as well as two other filters for direct imaging of the Sun. Mini-TES (*5*) produces high spectral resolution (10 $cm^{-1}$) infrared image cubes with a wavelength range of 5 to 29 μm. The Pancam cameras and the Mini-TES scanning mirrors are mounted atop a mast (*3*) at a height of ~1.5 m above the ground.

Once potential science targets have been identified using Pancam and Mini-TES, they have been studied in more detail with the use of two in situ compositional sensors mounted on a 5-degree-of-freedom robotic arm (*3*). These are an Alpha Particle–X-Ray Spectrometer [APXS (*6*)] and a Mössbauer Spectrometer (*7*). Radioactive $^{244}Cm$ alpha sources and two detection modes (alpha and x-ray) in the APXS reveal elemental abundances of rocks and soils (*8*). The Mössbauer Spectrometer measures the resonant absorption of gamma rays produced by a $^{57}Co$ source to determine splitting of nuclear energy levels in $^{57}Fe$ atoms, revealing the mineralogy and oxidation state of Fe-bearing phases. The instrument arm also carries a Microscopic Imager [MI (*9*)] that has been used to obtain high-resolution (30 μm/pixel) images of rock and soil surfaces and a Rock Abrasion Tool [RAT (*10*)] that can remove up to ~5 mm of material over a circular area 45 mm in diameter. Finally, the payload includes the Magnetic Properties Experiment consisting of seven magnets that have attracted fine-grained magnetic materials for viewing by payload instruments (*11*).

The rover itself uses a six-wheel rocker-bogie suspension system and onboard autonomous navigation and hazard avoidance capability, allowing traverse distances of tens of meters per sol (*1*). Navigation and hazard avoidance are aided by two monochromatic navigation cameras (Navcams) mounted on the mast, and by four hazard avoidance cameras (Hazcams) mounted in fore- and aft-facing stereo pairs on the rover body (*12*). Prelanding mission success criteria dictated that at least one of the rovers should travel a minimum of 600 m over its lifetime, with a goal of 1 km. The design surface lifetime for both vehicles was 90 sols.

The landing site chosen for Spirit lies within Gusev crater, a flat-floored crater that is 160 km in diameter and of Noachian age. The southern rim of Gusev is breached by Ma'adim Vallis, one of the largest branching valley networks on the planet. Gusev is expected to have acted as a settling pool for sediment carried by the water that cut Ma'adim before it overflowed and exited through a gap in the northern rim of the

[1]Department of Astronomy, Cornell University, Ithaca, NY 14853, USA. [2]Department of Earth and Planetary Sciences, Washington University, St. Louis, MO 63130, USA. [3]Abteilung Kosmochemie, Max-Planck-Institut für Chemie, Postfach 3060, D-55128 Mainz, Germany. [4]NASA Ames/SETI Institute, Moffett Field, CA 94035, USA. [5]Department of Geological Sciences, University of Nevada, Reno, NV 89557, USA. [6]U.S. Geological Survey, Menlo Park, CA 94025, USA. [7]Department of Geological Sciences, Arizona State University, Tempe, AZ 85287, USA. [8]Lockheed Martin Corporation, Littleton, CO 80127, USA. [9]New Mexico Museum of Natural History and Science, Albuquerque, NM 87104, USA. [10]NASA Ames Research Center, Moffett Field, CA 94035, USA. [11]Centre d'Etude Spatiale des Rayonnements, 31028 Toulouse Cedex 4, France. [12]Enrico Fermi Institute, University of Chicago, Chicago, IL 60637, USA. [13]Space Science Institute, Boulder, CO 80301, USA. [14]Jet Propulsion Laboratory, California Institute of Technology, Pasadena, CA 91109, USA. [15]Honeybee Robotics, New York, NY 10012, USA. [16]Center for Earth and Planetary Studies, Smithsonian Institution, Washington, DC 20560, USA. [17]Department of Earth, Atmospheric and Planetary Sciences, Massachusetts Institute of Technology, Cambridge, MA 02139, USA. [18]U.S. Geological Survey, Flagstaff, AZ 86001, USA. [19]Max-Planck-Institut für Aeronomie, D-37191 Katlenburg-Lindau, Germany. [20]Johannes Gutenberg-Universität, Staudinger Weg 9, D-55099 Mainz, Germany. [21]Botanical Museum, Harvard University, Cambridge, MA 02138, USA. [22]NASA Glenn Research Center, Cleveland, OH 44135, USA. [23]Department of Atmospheric Sciences, Texas A&M University, College Station, TX 77843, USA. [24]Department of Civil and Environmental Engineering and Geodetic Science, Ohio State University, Columbus, OH 43210, USA. [25]Niels Bohr Institute, Ørsted Laboratory, DK-2100 Copenhagen 0, Denmark. [26]Malin Space Science Systems, San Diego, CA 92191, USA. [27]Department of Geosciences, State University of New York, Stony Brook, NY 11794, USA. [28]Department of Earth and Planetary Sciences, University of Tennessee, Knoxville, TN 37996, USA. [29]NASA Johnson Space Center, Houston, TX 77058, USA. [30]Institut für Raumsimulation, Deutschen Zentrum für Luft- und Raumfahrt (DLR), Dj-51170 Köln, Germany. [31]NASA Goddard Space Flight Center, Greenbelt, MD 20771, USA. [32]Lunar and Planetary Laboratory, University of Arizona, Tucson, AZ 85721, USA. [33]Department of Physics, University of Alabama, Birmingham, AL 35294, USA. [34]Space Science Institute, Martinez, GA 30907, USA.

*To whom correspondence should be addressed. E-mail: squyres@astro.cornell.edu

crater. Exploration of the floor of Gusev therefore was anticipated to offer opportunities to study sediments that were derived from the southern highlands of Mars and deposited in a lacustrine environment (*13*).

Given the great length and depth of Ma'adim Vallis and the shallow depth and flat floor of Gusev crater, the quantity of lacustrine sediments filling the crater is likely to be substantial (*14*–*16*). The aqueous sedimentation events at Gusev probably occurred more than 3 billion years ago, however, and we recognized before landing that any water-lain deposits could have been buried by more recent volcanic and/or eolian materials (*13*). Small impact craters are common across the floor of Gusev, and the interiors and ejecta of such craters may provide access to material from stratigraphic horizons below the surface. The floor of Gusev also has a number of small hills, possibly erosional remnants that could preserve higher stratigraphic horizons that were never buried or were exhumed. We therefore anticipated that the rover's mobility could be important in accessing crater and hill material at the Gusev site that might be different from whatever materials dominate the plains.

**The Rover traverse.** Spirit touched down in the eastern portion of the Gusev crater landing ellipse, at a latitude of 14.5692°S and a longitude of 175.4729°E as defined in the planetocentric IAU 2000 coordinate frame (Fig. 2). The landing site, now named Columbia Memorial Station (*17*), lies in a region of locally low albedo on the floor of Gusev crater that we interpret to be a zone that has seen recent removal of some fine, loose particulates by dust devils. The first Navcam images of the site (Fig. 3) revealed a rock-strewn plain with low hills on the horizon. The largest impact crater within Spirit's reach, which we observed in the first Pancam panorama (Plate 1), was the Bonneville (*18*) impact crater (about 210 m in diameter), which lies about 300 m to the northwest of Columbia Memorial Station. The highest hills within Spirit's possible reach, the Columbia Hills (Plate 4), have summit altitudes about 100 m above the plains and lie about 2.6 km to the southeast of the landing site.

During the first 11 sols, we acquired full panoramas of the scene around the lander with Pancam (*19*) and Mini-TES (*20*). Egress from the lander took place on sol 12. After a brief initial investigation of the soil immediately adjacent to the lander with all of the instruments on the arm (*21*–*23*), we drove Spirit on sol 15 to the nearest large (~50 cm wide) rock, Adirondack (Plate 9). We then investigated Adirondack with all of the arm instruments, including use of the RAT to brush and abrade the rock surface (Plate 9B). Because of a flight software anomaly that occurred on sol 18, temporarily halting normal science operations, we did not command Spirit to drive away from Adirondack until sol 36.

The traverse path of Spirit from Columbia Memorial Station through the end of the nominal mission on sol 91 (Plate 14) consisted of a drive toward the northeast to the rim of Bonneville crater, in situ investigation of the Bonneville rim region and remote sensing of the crater floor, and then a turn toward the southeast and the beginning of the long drive toward the Columbia Hills. The traverse to and then away from Bonneville yielded the first transect through the ejecta deposits of an impact crater on another planet. Along the way we made several extended stops during which we investigated high-priority science targets with the full Athena payload. In addition, all traverse sols included the use of Pancam and Mini-TES, and many also included brief "touch and go" measurements with the MI, APXS, and/or Mössbauer Spectrometer on targets of opportunity (*3*).

Spirit drove away from Adirondack on sol 36, arriving at a low circular depression (probably a small impact crater) named Laguna Hollow on sol 45. During sols 46 to 49 we used the rover's wheels to excavate a trench in the soil of Laguna Hollow (Plate 7). We resumed the drive toward Bonneville on sol 50, stopping on sol 54 at a large boulder named Humphrey (Plate 10A). Sols 55 to 60 were spent investigating Humphrey in detail, including brushing (Plate 10B) and grinding (Plate 10C) with the RAT, acquisition of compositional data at several steps in the process, and acquisition of a mosaic of MI images (Plate 12). We resumed the drive toward the rim of Bonneville on sol 61, and arrived there on sol 67 (Plate 3).

Sols 68 to 77 were spent performing detailed remote sensing with Pancam (Plate 5) and Mini-TES (Plate 6) of the interior of Bonneville, as well as exploration of the Bonneville rim that included trenching and in situ

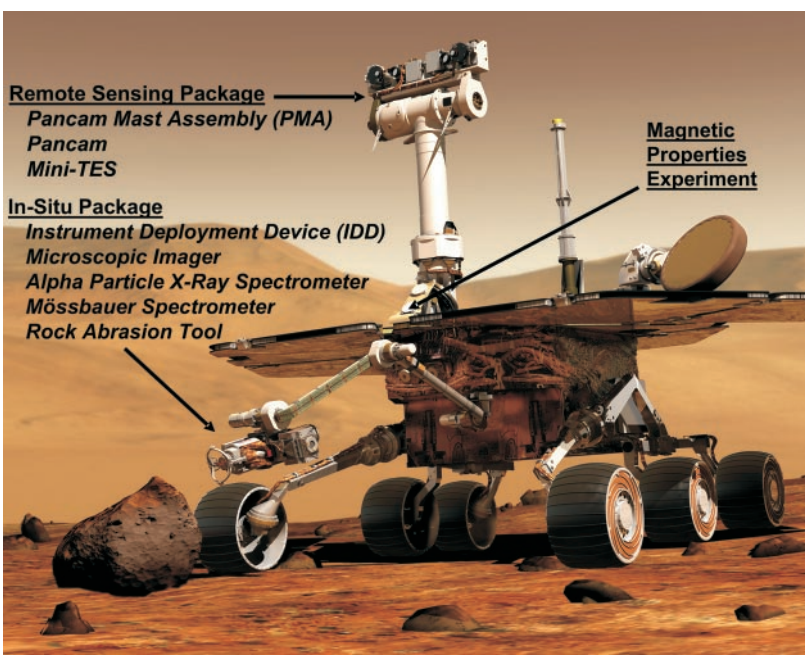


**Fig. 1.** The MER rover, showing the location of the various elements of the Athena science payload.

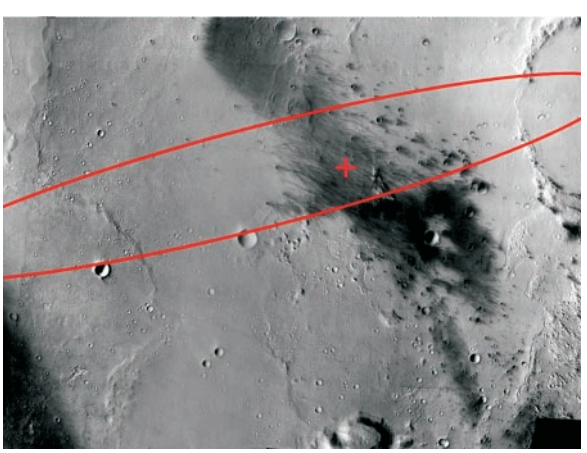

**Fig. 2.** A Mars Odyssey THEMIS (Thermal Emission Imaging System) visible-wavelength image of the floor of Gusev crater, showing the location of the Spirit target ellipse and the actual landing location (cross). Scale across the image is ~70 km.

investigation of an eolian drift named Serpent. Because the remote sensing of Bonneville did not reveal features within the crater that merited detailed investigation, we turned Spirit toward the southeast and the Columbia Hills. Sols 78 to 86 were spent performing a detailed analysis, with the full payload, of a light-toned rock named Mazatzal (Plates 11A to 11C, Plate 13). Through the end of the nominal mission at sol 91, we continued to drive Spirit toward the Columbia Hills.

The path of the traverse was documented using the navigation capabilities aboard the rover. Localization experiments included triangulation based on landmarks seen on the horizon in Pancam and Navcam images, together with a formal least-squares bundle adjustment using features delineated in overlapping images, wheel odometry, rover gyro and accelerometer data, and Pancam observations of the Sun (*24*). Results indicate that the total length of the rover traverse during the 90-sol primary mission was 637 m as measured by wheel odometry, 506 m as assessed from formal localization performed for the locations where image data were acquired, and 316 m by straight-line distance.

**Soils.** The soils on the Gusev crater plains explored by Spirit are ubiquitous; they cover flat regions as well as depressions that we have termed hollows (see below), and also exist as discrete drifts of probable eolian origin (*24*–*26*). A thin cover of dust-sized particles of likely airborne origin covers much of the soil and rocks observed around Columbia Memorial Station and during traverses to and from the rim of Bonneville crater. Mini-TES emissivity spectra show that the dust cover rather closely mimics the typical dust spectrum retrieved from Mars Global Surveyor (MGS) TES data (*20*), and 11-color Pancam reflectivity spectra of the dust cover are consistent with previous telescopic and spacecraft measurements of classical bright regions (*19*). Exceptions to the dust-covered soils include inferred upwind sides of some drifts that expose darker materials, presumably because of preferential scouring on these drift faces. The thin nature of the dust cover on soils is evident from examination of rover tracks that commonly expose underlying darker materials (e.g., Plate 2). Microscopic imaging of undisturbed soils suggests that the dust deposits exist as aggregates of finer particles (*21*). The continuing nature of dust accumulation is evident from monitoring the degradation of power with time from the solar panels, in addition to slight reddening of the Pancam calibration target and other components on the rover deck (*19*). A mean decrease in solar array energy output of 0.2% per sol is inferred over the 90-sol primary mission (*24*).

The composition of Gusev soils determined from Spirit APXS data is similar to the composition determined from measurements at the Pathfinder and Viking sites (*22*), consistent with homogenization of soils by wind on regional and global scales. Sulfur and chlorine are enhanced relative to fresh rock surfaces at Gusev, although the bulk soil compositions are dominated by basaltic materials. Mössbauer observations of soils show the presence of olivine, pyroxene, and magnetite, as well as oxidized iron phases (containing $Fe^{3+}$, ferric iron) (*23*). In addition, low concentrations of carbonates and sulfates are implied by Mini-TES data (*20*). Mini-TES data for dark soils exposed in wheel tracks, in the dark materials in the trench excavated in Laguna Hollow, and in the disturbed areas in Serpent drift show basaltic signatures typical of those inferred for selected dark areas from MGS TES data (*20*, *24*). Pancam spectra of soils are also consistent with fine-grained, ferric-rich, poorly crystalline phases (*19*).

Soils disturbed during landing by retraction of the airbags, by traversing, and during trenching and scuffing by the wheels tend to look cloddy, implying some cohesive strength in the upper few centimeters (*24*). Sources of cohesion may include a small amount of cementation or electrostatic forces between soil particles. The Laguna Hollow trench suggests cohesion to the depth of the trench, which was about 6 to 7 cm. The composition of the trench interior is similar to the undisturbed surface, except for a lower ferric iron oxide content, consistent with a layer of more ferric iron–rich dust on the surface than in the subsurface (*19*).

Grain sizes for soils inferred from Mini-TES thermophysical measurements (e.g., Plate 6) suggest that the hollows are filled with the finest grained materials, with an average particle size in the silt to fine-sand range (*20*). Drifts are seen from imaging data to be covered with a monolayer of particles with medium to coarse sand sizes. This layer appears to be an armor that protects the bedform from erosion and redeposition. There is also a suggestion in some of the highest resolution Pancam images of the plains near Columbia Memorial Station that rock clasts are sitting on a coarse sand layer, with both materials variably covered with dust (Fig. 4).

**Rocks.** Dark, fine-grained rocks, many of them vesicular, litter the Spirit landing site. Many rocks are variably mantled with high-albedo material. Although many of the rocks observed along Spirit's traverse during the

**Fig. 3.** The first image of the martian surface acquired by Spirit. It is a Navcam image acquired on sol 1, reduced in resolution to 512 × 512 pixels and obtained before deployment of the Pancam Mast Assembly. (Image ID 2N126467960)

nominal mission were probably excavated from Bonneville crater, no breccias or obvious shock effects have been noted in any images.

Rocks are variably coated with bright materials, particularly on flat facets and on low rocks that are partially embedded in soils and have been shaped by the wind. Some rocks (e.g., Adirondack, Plate 9) have a distinctive two-toned appearance; upper portions look relatively fresh and dark, whereas lower portions are brighter and coated. Other rocks, particularly ones with upper surfaces that lie close to ground level, are completely covered with bright coatings (e.g., Mazatzal, Plate 11A).

Pancam and Mini-TES spectra of the dark surfaces of all rocks at the Gusev site observed to date are consistent with the spectra of basaltic rocks (*19*, *20*). The texture and composition of Adirondack, Humphrey, and Mazatzal were analyzed using the full Athena payload, including use of the RAT to produce brushed and abraded surfaces.

These rocks are volcanic materials of basaltic composition (*27*). Rock interiors viewed in MI images contain dark megacrysts, possibly olivine (Plates 12 and 13). The presence of olivine is confirmed by Mössbauer spectra (*23*); these spectra also reveal pyroxene and magnetite. Rock compositions extrapolated from APXS spectra of natural, brushed, and abraded APXS measurements correspond to olivine-rich basalts (*22*). Calculated norms, which conform to the redox state measured by the Mössbauer Spectrometer, suggest that the rocks contain olivine, plagioclase, and pyroxenes, with accessory magnetite, ilmenite, and phosphate. The normative mineral compositions are similar to those in basaltic martian meteorites, although the bulk chemical compositions are different. Basaltic lavas at Gusev may have formed by partial melting of an ancient mantle source that was not previously depleted by formation of the crust.

The rocks also show evidence of fractures and vugs filled to varying degrees with bright materials, perhaps of aqueous origin. Pancam and MI images of Mazatzal show unambiguous evidence of multiple coatings: a dark, smooth layer sandwiched between two thin, light-toned layers (Plate 13). MI images of an oblique RAT cut into Humphrey reveal a subsurface layer with distinct fine-grained texture (Plate 12). These coatings probably represent alteration, as do veins, filled fractures, and amygdules in the interiors of three separate rocks. APXS chemical compositions of the alteration materials are distinct from those of the rock interiors and do not lie along mixing lines between rock and Gusev soils (*22*). The dark coating on Mazatzal and the higher albedo materials seen in the interiors of all three rocks may result from reactions with aqueous fluids; light coatings on rock exteriors could be cemented dust.

The three rocks that were abraded by the RAT required grinding energy per unit volume that suggests mechanical strengths somewhat less than those of hard terrestrial basalts (*24*). This finding is also consistent with the view that the outer portions of these rocks have undergone some degree of alteration.

**Geologic processes.** Evolution of the surface materials that we have observed at Gusev crater has been dominated by impact processes. Impact craters ranging in size from a few meters to hundreds of meters and larger (e.g., Thyra crater, located ~20 km to the east) are responsible for much of the low relief on the plains and for the blocky rubble that mantles the surface. Shallow circular depressions, or hollows, represent the smallest, most modified members of the crater population. Formation of the hollows and emplacement of associated ejecta (recognized as accumulations of blocks on and distal to the hollow rims) have disrupted the surface, promoting erosion by the wind, deflating the surface and leaving perched rocks in the ejecta. Hollow interiors have experienced geologically rapid modification, as demonstrated by trenching that revealed uniform infilling by comparatively unaltered and dust-free sediments that may bury many rocks.

Ejecta deposits associated with Bonneville were seen along the traverse, and surface expression of the ejecta is in line with expectations for a relatively pristine impact structure (*28*). Most of the ejecta clasts retain angular to subangular shapes. Rock abundance and rock size increase toward the rim of Bonneville by factors of approximately 2 and 5, respectively. The largest blocks are more than 2 m in their longest dimension, which suggests that they were impact-fragmented from blocks as large as 6 to 7 m in length and at least 10 m beneath the gardened regolith surface (*29*).

Wind-related features observed at Gusev include depositional features such as ripples and mantles of dust on rocks, as well as erosional features on rocks, such as beveled sides, facets, and grooves (Fig. 5). Wind-blown sediments include dust, sand, and granules. Bedforms consist primarily of meter-size ripples in which the crests have a surface layer of well-rounded coarse sands and the troughs consist of poorly size-sorted sands. MI images show that the sands have a bimodal size distribution (*21*), with modes centered on fine sand (0.1 to 0.3 mm in diameter) and coarse sand to granules (1 to 3 mm in diameter). The larger grains are subangular to rounded, and appear to be lithic fragments. The presence of surface crusts on the deposits and bedforms, the inclusion of dust on the bedforms, and the absence of sand dunes and steep slip faces all suggest that the sand is not currently active.

Wind direction indicators are abundant. The axes of ripples and other bedforms are oriented east-northeast to west-southwest and are slightly asymmetric with the steeper slope on the east-southeast side, suggesting formative winds from the west-northwest. Lower albedo portions of most drift deposits and rocks face west-northwest. Drift deposits around some rocks—indicators of wind directions similar to ones seen at the Mars Pathfinder site (*30*)—are tapered toward the southeast. Wind-abraded rocks (ventifacts, Fig. 5)

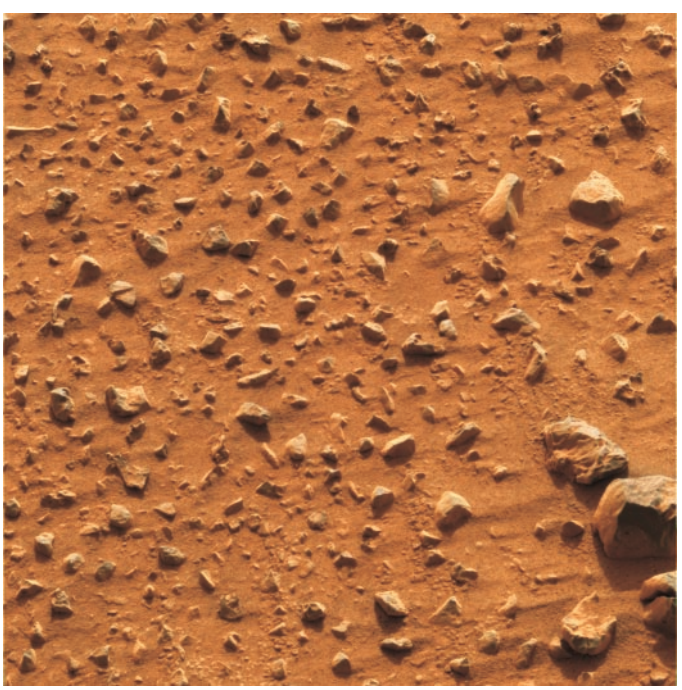

**Fig. 4.** A Pancam color image of soil in Gusev crater, showing regularly spaced clasts and coarse sand, all coated with dust. The image was acquired on sol 12 at around 15:30 LST, using the Pancam's L2 (750 nm), L5 (530 nm), and L6 (480 nm) filters, and is an approximate true-color rendering. Scale across the image is ~50 cm. (Image ID 2P127444032)

suggest formative winds from the northwest. RAT operations on Adirondack and Humphrey produced rock cuttings that were asymmetrically distributed toward the southeast (Plates 10 and 11). All of these results are consistent with predictions (*31*) of afternoon winds in Gusev crater that blow from the northwest, and with the analysis of the orientations of wind-related features seen from orbit (*32*).

Many of the rocks at the Gusev site show evidence for partial or complete burial followed by exhumation. These include the two-toned rocks discussed above, ventifacts that originate from a common horizon (suggesting that the lower part of the rock was shielded), and rocks that appear to be perched on top of other rocks. In addition, some rocks appear to be undercut (i.e., the soil has been removed from beneath their edges). Taken together, these observations suggest that surface deflation, perhaps highly localized, of 5 to 60 cm has occurred.

Eolian activity clearly has been subordinate to impacts in shaping the surface. The dominant role of impact has contributed to destruction or burial of any primary morphology associated with alluvial or lacustrine infilling of Gusev crater. Moreover, the pristine basaltic lithology and the absence of evidence for phyllosilicates or other aqueous weathering products in the Mini-TES, APXS, and Mössbauer data argue either that water-lain deposits are absent from surficial deposits or that any association with standing water was short-lived.

Although volcanic materials dominate the deposits observed at Gusev, no obvious volcanic source has been identified, either from the surface or from orbit. Instead, the rocks may be derived from lavas that are inferred to cover the floor of Gusev farther to the northeast (*33*) and may also have extended into the landing region, where they were later disrupted by impact. We have observed a few rocks whose textures resemble a'a and pahoehoe, the characteristic forms of lava flow surfaces seen at young terrestrial volcanoes such as Kilauea; again, these findings are consistent with substantial impact disruption and mixing.

**Comparison to landing site predictions.** Prelanding predictions of the physical properties of the Gusev landing site (*13*) are broadly consistent with our observations. The landing location has a bulk TES thermal inertia of 300 to 350 J $m^{-2}$ $s^{-0.5}$ $K^{-1}$, suggesting a surface dominated by duricrust to cemented soil-like materials or cohesionless sand and granules, which is consistent with the observed thermal inertias and soil characteristics at Gusev (*20*, *21*). Spirit landed in the darkest portion of the Gusev landing ellipse (albedo ~0.19) characterized by dust devil tracks, and then traversed into a higher albedo area that included Bonneville (albedo ~0.26). The albedo measured by Pancam is comparable (*19*), which suggests that albedo in Gusev can be used as a proxy for the amount of bright atmospheric dust on the surface. The rock abundance derived from orbital thermal differencing techniques at the Gusev landing site is ~7%, similar to rock counts within 10 m of Columbia Memorial Station that yield ~5%. This value is within the ±5% uncertainty of the orbital estimate (*34*), although the abundance of rocks has varied by perhaps factors of 2 to 4 along the nominal mission traverse. Orbital estimates of slope at scales of 1 km and 100 m (from Mars Orbiter Laser Altimeter topography) and 5 m (from Mars Orbiter Camera stereogrammetry and photoclinometry and from radar roughness) indicate that Gusev is comparable to or smoother than the Viking Lander 1 and Mars Pathfinder sites at all three scales (*13*), consistent with the relatively flat and moderately rocky plain seen in the Pancam and Navcam images.

**Atmospheric science.** Upward-looking Mini-TES spectra reveal the vertical thermal structure of the atmosphere between about 20 and 2000 m above the surface, as well as column-integrated infrared aerosol optical depth, water vapor abundance, and aerosol particle size. The retrieved temperature profiles show the development of a near-surface superadiabatic layer during the afternoon and a deep inversion layer at night (Fig. 6). Upward-looking Mini-TES stares, in which spectra are collected every 2 s for up to an hour, show warm and cool parcels of air moving through the Mini-TES field of view on a time scale of 30 s.

Direct solar imaging with Pancam provides a measurement of visible-wavelength optical depth, whereas near-Sun and sky brightness surveys help reveal the physical

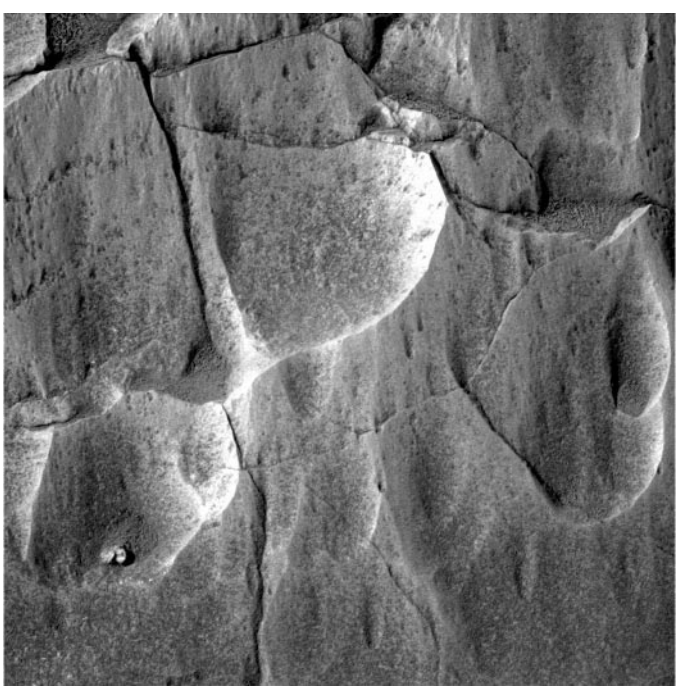

**Fig. 5.** A Pancam image of ventifacts on the wind-scoured surface of the rock Mazatzal. The image was acquired on sol 78 at around 10:40 LST using the Pancam's L7 (1000 nm) filter. Scale across the image is ~50 cm. (Image ID 2P133283852)

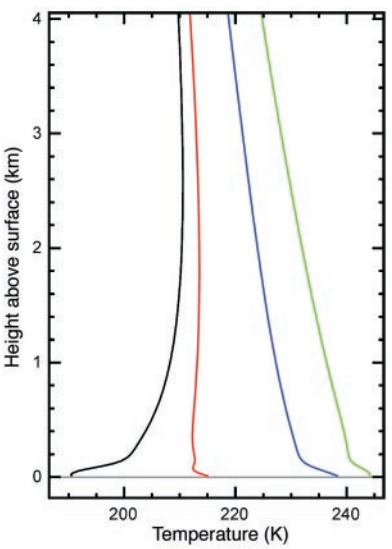


**Fig. 6.** Atmospheric temperature as a function of height above the surface, as observed by Mini-TES. Temperature profiles were taken on sol 72, 12:55 hours (blue); sol 73, 05:20 hours (black); sol 73, 10:00 hours (red); and sol 73, 15:45 hours (green). There is a large diurnal variation in atmospheric temperatures, especially near the surface. In the afternoon (blue and green profiles), near-surface temperatures drop very rapidly with height, forming a superadiabatic layer more than 100 m deep; at night (black profile), strong surface cooling leads to an inversion layer at least 2 km thick. The mini-TES instrument is sensitive to atmospheric temperatures up to about 2 km above the surface. Temperatures above that height are based on concurrent MGS TES observations (*35*).

properties, scattering properties, and vertical structure of particles suspended in the atmosphere. We have monitored the fallout of dust after a large regional dust storm that occurred in December 2003 and the further clearing associated with the transition into the southern hemisphere fall season (*35*). Visible-wavelength dust optical depth at Gusev crater dropped from a value of 0.90 soon after landing to 0.56 on sol 91.

**Magnetic properties.** Each rover carries three permanent magnets designed to attract dust from the martian atmosphere, as well as four small magnets designed to attract rock dust produced during RAT operations. Pancam observations of these magnets indicate that particles fine enough to be suspended in the martian atmosphere are typically composed of more than one mineral phase, and that most of the particles, perhaps all of them, are magnetic in the sense that they are attracted to permanent magnets (*36*). A ferrimagnetic mineral (magnetite, titanomagnetite, or maghemite), present at about 2 weight percent in the dust collected, is most consistent with the observations. Hematite alone cannot be responsible for the magnetism of the dust particles. The fact that the RAT magnets collected low-albedo dust during grinding suggests that the rocks contain substantial ferrimagnetic mineral, consistent with the Mössbauer observations of magnetite.

**Summary.** Gusev crater was chosen as the landing site for Spirit because there is evidence that it once contained a lake (*13*). However, to date we have found no evidence for lacustrine sedimentation at the Spirit landing site. The morphologic, lithologic, and mineralogic features observed can be explained by local impact disruption of volcanic rocks, followed by eolian modification. Any lacustrine sediments at Gusev were buried by volcanic activity, and Spirit to date has sampled only the impact-disrupted products of this volcanism, plus soils that represent a mixture of locally derived and globally mixed fine-grained materials.

We cannot rule out the possibility that some of the materials that we have observed at the Spirit landing site were transported into Gusev by water that flowed through Ma'adim Vallis. Many of the rocks at our landing site are small enough to have been transported into Gusev via some kind of hyperconcentrated, water-charged debris flow. However, we have seen little direct evidence (e.g., rounded blocks, imbrication, percussion marks, block-to-block variations in lithology) to support this view. Moreover, the obvious relationships between block properties and distance from Bonneville crater clearly implicate impact as important, if not dominant, in producing the block distributions that we see.

It is also plausible that fluvial/lacustrine processes transported fine-grained sediments as far into Gusev crater as our landing site. These materials may have remained unconsolidated after deposition, never forming sedimentary rocks, and they may have mixed with volcanic fragments by impact processes. If so, then some of the fine-grained soils that we see may actually be sediments that were transported by fluvial processes into Gusev crater. We have seen no direct evidence to support this hypothesis, however.

Regardless of whether fluvial or lacustrine processes have played any role in emplacement of the rocks and soils that we have seen, water probably has been involved (although to a limited degree) in the formation of the veins, filled vugs, and surface coatings that are associated with rocks at the Spirit landing site. This view is particularly supported by the high concentrations in the veins, vugs, and coatings of elements such as S, Cl, and Br that are easily mobilized by water. The light-toned coatings on some rocks may have formed while the low-lying portions of rocks were buried by drift migration or by frost deposited in periods of high obliquity. In such a scenario, as water migrated upward by capillary action between soil grains or along rock surfaces, evaporation left salts behind that acted as cementing and coating agents on rock surfaces.

### References and Notes


1. J. A. Crisp *et al*., *J. Geophys. Res*. **108**, 8061, doi: 10.1029/2002JE002038 (2003).
2. A martian solar day has a mean period of 24 hours 39 minutes 35.244 seconds, and is referred to as a sol to distinguish this from a roughly 3% shorter solar day on Earth. A martian sidereal day, as measured with respect to the fixed stars, is 24h 37m 22.663s, as compared with 23h 56m 04.0905s for Earth. See www.giss.nasa.gov/tools/mars24 for more information.
3. S. W. Squyres *et al*., *J. Geophys. Res*. **108**, 8062, doi:10.1029/2003JE002121 (2003).
4. J. F. Bell III *et al*., *J. Geophys. Res*. **108**, 8063, doi: 10.1029/2003JE002070 (2003).
5. P. R. Christensen *et al*., *J. Geophys. Res*. **108**, 8064, doi:10.1029/2003JE002117 (2003).
6. R. Rieder *et al*., *J. Geophys. Res*. **108**, 8066, doi: 10.1029/2003JE002150 (2003).
7. G. Klingelhöfer *et al*., *J. Geophys. Res*. **108**, 8067, doi:10.1029/2003JE002138 (2003).
8. The term martian soil is used here to denote any loose, unconsolidated materials that can be distinguished from rocks, bedrock, or strongly cohesive sediments. No implication of the presence or absence of organic materials or living matter is intended.
9. K. E. Herkenhoff *et al*., *J. Geophys. Res*. **108**, 8065, doi:10.1029/2003JE002076 (2003).
10. S. Gorevan *et al*., *J. Geophys. Res*. **108**, 8068, doi: 10.1029/2003JE002061 (2003).
11. M. B. Madsen *et al*., *J. Geophys. Res*. **108**, 8069, doi:10.1029/2002JE002029 (2003).
12. J. Maki *et al*., *J. Geophys. Res*. **108**, 8071, doi: 10.1029/2003JE002077 (2003).
13. M. P. Golombek *et al*., *J. Geophys. Res*. **108**, 8072, doi:10.1029/2003JE002074 (2003).
14. N. A. Cabrol, E. A. Grin, G. Dawidowicz, *Icarus* **123**, 269 (1996).
15. N. A. Cabrol, E. A. Grin, R. Landheim, *Icarus* **132**, 362 (1998).
16. N. A. Cabrol, E. A. Grin, R. Landheim, R. O. Kuzmin, R. Greeley, *Icarus* **133**, 98 (1998).
17. Columbia Memorial Station was named to honor the crew of Space Shuttle Columbia, who perished on 1 February 2003. The name Columbia Memorial Station refers both to the lander itself and to the martian terrain that it occupies.
18. Names have been assigned to areographic features by the Mars Exploration Rover (MER) team for planning and operations purposes. The names are not formally recognized by the International Astronomical Union.
19. J. F. Bell III *et al*., *Science* **305**, 800 (2004).
20. P. R. Christensen *et al*., *Science* **305**, 837 (2004).
21. K. E. Herkenhoff *et al*., *Science* **305**, 824 (2004).
22. R. Gellert *et al*., *Science* **305**, 829 (2004).
23. R. V. Morris *et al*., *Science* **305**, 833 (2004).
24. R. E. Arvidson *et al*., *Science* **305**, 821 (2004).
25. J. A. Grant *et al*., *Science* **305**, 807 (2004).
26. R. Greeley *et al*., *Science* **305**, 810 (2004).
27. H. Y. McSween *et al*., *Science* **305**, 842 (2004).
28. J. A. Grant, P. H. Schultz, *J. Geophys. Res.* **98**, 11025 (1993).
29. H. J. Melosh, *Impact Cratering* (Oxford Univ. Press, Oxford, 1989).
30. R. Greeley *et al*., *J. Geophys. Res*. **104**, 8573 (1999).
31. S. R. C. Rafkin, T. I. Michaels, *J. Geophys. Res*. **108**, 8091, doi:10.1029/2002JE002027 (2003).
32. R. Greeley *et al*., *J. Geophys. Res*. **108**, 8077, doi: 10.1029/2002JE002006 (2003).
33. K. A. Milam *et al*., *J. Geophys. Res*. **108**, 8078, doi: 10.1029/2002JE002023 (2003).
34. P. R. Christensen, *Icarus* **68**, 217 (1986).
35. M. D. Smith, *Icarus* **167**, 148 (2004).
36. P. Bertelsen *et al*., *Science* **305**, 827 (2004).


37. We are deeply indebted to the many hundreds of engineers and scientists—far too numerous to name here—who made the Mars Exploration Rover Project and the Athena Science Investigation possible. Funding for the MER Project, including most of the Athena payload, was provided by NASA. The APXS and Mössbauer instruments were funded by the German Aerospace Center (DLR), and the magnet array was funded by the Danish government. The MER Project was led with skill and dedication by P. Theisinger, and the development of the MER flight system was led with equal skill and dedication by R. Cook and B. Goldstein. J. Rademacher managed the development of the Mini-TES, APXS, and Mössbauer payload elements, M. Schwochert led the engineering teams for Pancam and the Microscopic Imager, and S. Kondos and M. Johnson managed the development of the Rock Abrasion Tool. To all of them, and to the hundreds of members of the MER family who have made this adventure such a joy and privilege to be part of, we express our heartfelt and lasting thanks.


**Plates Referenced in Article**

www.sciencemag.org/cgi/content/full/305/5685/794/DC1

Plates 1 to 7 and 9 to 14

11 May 2004; accepted 9 July 2004